JOURNAL OF AIRCRAFT
Vol. 33, No. 3, May–June 1996

Engineering Notes

ENGINEERING NOTES are short manuscripts describing new developments or important results of a preliminary nature. These Notes cannot exceed 6 manuscript pages and 3 figures; a page of text may be substituted for a figure and vice versa. After informal review by the editors, they may be published within a few months of the date of receipt. Style requirements are the same as for regular contributions (see inside back cover).

Optimal Rectangular End Plates

D. W. F. Standingford* and E. O. Tuck†
University of Adelaide, Adelaide 5005, Australia

Nomenclature

A = total area, wing plus end plates
A_0 = wing area
a = horizontal end plate offset
b = vertical end plate offset
C_L = lift coefficient based on A, $L/(\frac{1}{2}\rho U^2 A)$
C_L^0 = lift coefficient based on A_0, $L/(\frac{1}{2}\rho U^2 A_0)$
c = wing chord
h = end plate height
L = lift
l = end plate length
s = wingspan
U = freestream airspeed
α = angle of attack
ρ = fluid density

Introduction

WITHIN thin-wing theory[1] the problem of determining the lift L on a wing–end plate combination at small angle of attack α in a uniform stream U of air of constant density ρ relies on the solution of a pair of coupled singular integral equations[2] for the bound vorticity distribution on both wing and end plate. This is just the generalization of the usual lifting surface integral equation[1] to include the induced downwash of the wing on the end plate and vice versa. These integral equations have been solved numerically here, using modifications[3] to the constant-vorticity panel method of Tuck.[4]

These modifications improve the numerical resolution of the leading edge and wingtip singularities for the basic panel method, which is already significantly better than the vortex lattice method.[5] It is particularly important to achieve a good resolution of these singularities for the present task, because numerical artifacts such as overestimation of the loading at the leading edge can wrongly favor end plates located close to the leading edge. Similarly, there may appear to be a false local maximum in lift when the end plate is attached either completely above (or equivalently below) the wing, due to numerical error in resolving the wingtip singularity. Special care must be taken when the end plate dimensions are either small or large when compared with those of the wing, since there can be interference between the smaller element and the numerical panel scale of the larger element. Most results in the present Note were computed using a 12 × 12 rectangular Chebyshev-spaced grid on both the wing and end plate and are believed to be accurate to at least three significant figures.

Received June 22, 1995; revision received Aug. 26, 1995; accepted for publication Aug. 26, 1995.

*Postgraduate Student, Department of Applied Mathematics.
†Professor, Department of Applied Mathematics.

The complete parameter space for rectangular end plates on a rectangular wing of chord c and span s has been explored. That is, rectangular end plates of arbitrary length l and height h are placed on and perpendicular to both wingtips (i.e., side edges) of the rectangular wing, with their centers offset a horizontally and b vertically from the midpoint of the wingtip.

The aim is to maximize the lift coefficient per unit angle of attack C_L/α, based on the total (wing plus end plate) area A, by varying all four of the previous input plate parameters. In a rough sense, this is equivalent to maximizing lift/drag ratio, if drag is dominated by skin friction, and therefore, is proportional to the total area A. In a more general optimization, one would need to include induced drag; since this is proportional to α^2, the present results can be viewed as optimization at very small angles of attack.

Results

The effect of adding an end plate to a finite span wing is to inhibit spillage of air from the lower surface to the upper surface, via the tips. This then maintains the lift-creating pressure difference between bottom and top surfaces to a distance closer to the tips than if there were no end plates. Thus, the flow becomes more two dimensional, as if the wing's AR were larger, and the net lift increases.

Figure 1a shows the lift increase to a rectangular wing of various ARs s/c, obtained by adding an end plate with $a = b = 0$ and $l = c$, as a function of h. Thus, this end plate has the full wing chord and is attached flush, leading edge to leading edge and trailing edge to trailing edge. Note that for the purpose of this figure (and the next), the area measure is the area $A_0 = cs$ of the wing only, and these results do not penalize the lift for the extra area of the end plates; C_L^0/α is used to emphasize this distinction.

With this family of end plates, fully two-dimensional flow can never be attained even when h is infinite. Although the results reach distinct asymptotes as the end plate height increases for each fixed wing AR, the precise relationship between the asymptotic value for an infinitely high (but finite length) end plate and the wing parameters is not known. Of course, as the wing AR increases, the results approach the well-known two-dimensional value $C_L^0/\alpha = 2\pi$, and end plates provide relatively less benefit.

Since even quite small end plates have a dramatic effect on the square wing with $s/c = 1$, and there are applications (e.g., to dirt-track racing cars as in Ref. 6) where wings of approximately square planform are important, our attention from now on is confined to that case. The results in Fig. 1a for this case at large heights provide a numerical correction to preliminary results presented by Tuck.[2]

Figure 1b shows the variation with h of the lift (as C_L^0/α, based again on wing area only) for a square wing to which is added centrally placed (i.e., $a = b = 0$) end plates of various lengths l, fixed relative to c. Again, as h increases, these curves approach an asymptote whose value varies with end plate length, and only approaches the two-dimensional limit of 2π for large l/c, when the end plates become infinitely extended in both directions.

Although end plates increase the lift compared to a bare wing, this does not necessarily mean that the lift coefficient slope C_L/α as defined earlier based on total area A increases,

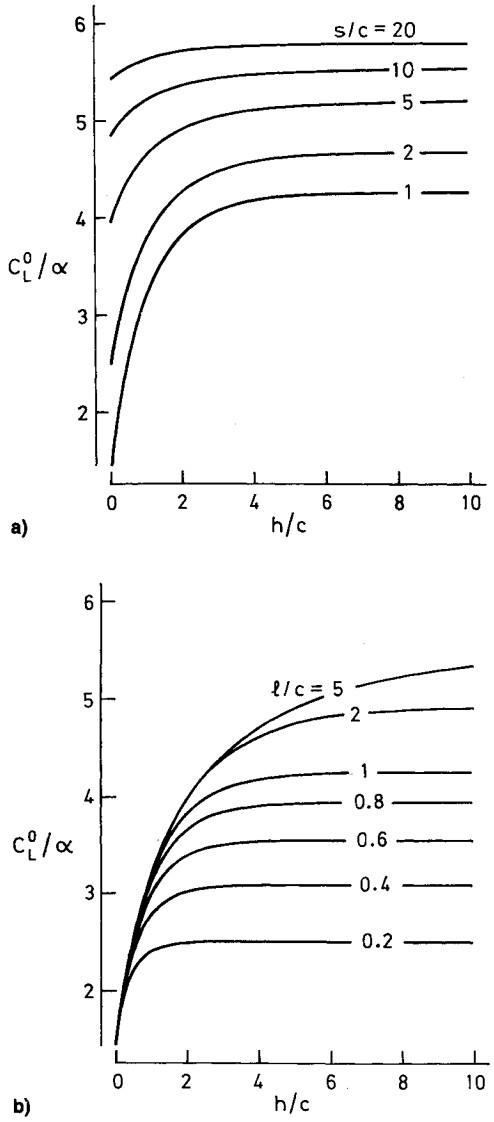

Fig. 1 C_L^0/α vs h/c for a) end plates with fixed length $l = c$ on rectangular wings of varying AR and b) end plates of varying l/c on a square wing.

since the end plates add to the total area, and hence, may have a negative affect on the lift/area ratio. Indeed, it is not difficult to see from the results of Fig. 1b that no end plate of length l equal to or greater than c produces a combined wing–end plate geometry with a $C_L\alpha$ value greater than that of a bare wing. However, it is a different story for shorter end plates.

The optimal dimensions and location of the end plate are shown via contour plots of C_L/α in Fig. 2. In Fig. 2a, the dimensions of the plate are fixed at $l = 0.5$ and $h = 0.5$ while the offsets a and b are varied. The clear maximum is when the plate is centered on the wing midchord, i.e., $a = b = 0$. Figure 2b has the offsets fixed at this optimum while the dimensions of the end plate vary. The maximum $C_L/\alpha = 1.84$ is attained when $l = 0.15c$ and $h = 0.48c$. In this figure, the axes $h = 0$ and $l = 0$ represent geometries where the end plate does not exist, and hence, they have contour value $C_L/\alpha = 1.46$ corresponding to the bare wing. There is another contour with this value that intersects the horizontal and vertical axes at $l/c = 1$ and $h/c = 3.1$, respectively. Any choice of h/c and l/c lying within the closed loop thus produced gives $C_L/\alpha > 1.46$, i.e., an improvement on the bare wing.

If one is forced to use a suboptimal placement of the end plates, i.e., nonzero a, b, then the optimal end plate dimensions depend upon the offset parameters a and b. Table 1 gives the

Table 1 Optimal end plate dimensions at fixed locations

a	b	Optimal l	Optimal h	Optimal C_L/α
$-c/2$	$h/2$	0.28	0.22	1.62
$-c/2$	0	0.25	0.36	1.67
0	$h/2$	0.19	0.28	1.71
0	0	0.15	0.48	1.84

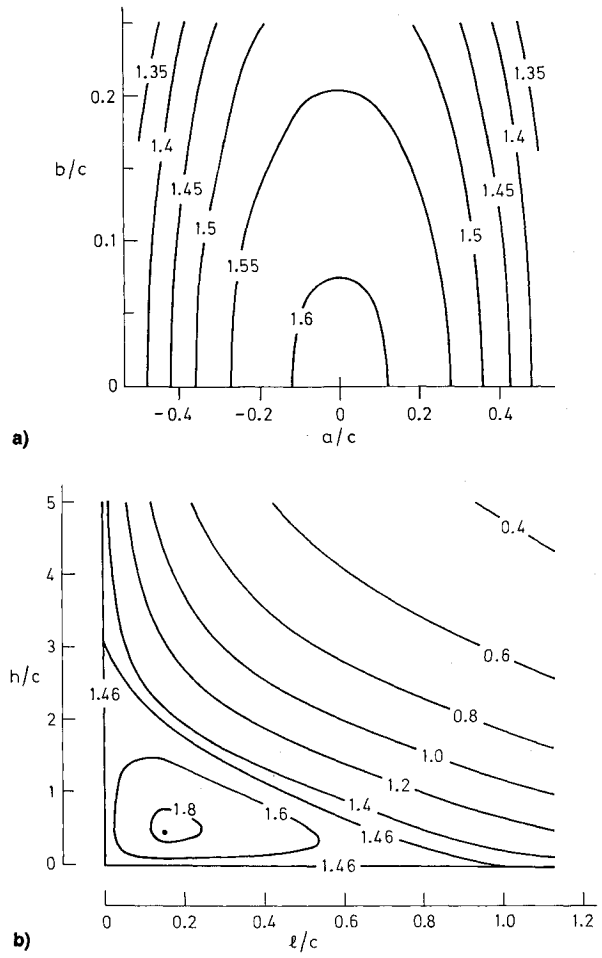

Fig. 2 Contour plots of C_L/α with a) end plate dimensions fixed at $l = 0.5c$ and $h = 0.5c$ and variable horizontal offset a and vertical offset b and b) the offsets fixed at $a = b = 0$ and variable plate dimensions.

optimal dimensions and the resulting lift coefficient slope when the end plate horizontal offset is $a = -c/2$ (flush with the wing leading edge) or $a = 0$ (horizontally centered at wing midchord), and the vertical offset is $b = h/2$ (entirely above wing) or $b = 0$ (vertically centered).

The bare square wing with no end plates has the value for C_L/α given in Tuck[4] to seven-figure accuracy as 1.460227. The final conclusion of this Note is that the same wing with end plates of length $l = 0.15c$ and height $h = 0.48c$, centered both horizontally and vertically at the midchord of the wing ($a = b = 0$) has $C_L/\alpha = 1.84$. If the extra area of magnitude $0.144c^2$ due to these two optimal end plates were instead added to the span of the previously square wing, so making a rectangular bare wing of AR $s/c = 1.144$, this wing would have only $C_L/\alpha = 1.63$. It is thus better to use this area in the form of (optimal) end plates rather than increased (full-chord) span.

References

[1]Ashley, H., and Landahl, L., *Aerodynamics of Wings and Bodies*, Addison–Wesley, New York, 1965, pp. 124–148.

[2]Tuck, E. O., "Lifting Surfaces with Endplates," *Proceedings of the 11th Australasian Fluid Mechanics Conference*, edited by M. R.

Davis and G. J. Walker, Univ. of Tasmania, Australia, 1992, pp. 219–222.
[3]Standingford, D. W. F., Lazauskas, L. V., and Tuck, E. O., "On the Numerics of the Lifting Surface Equation," Applied Mathematics Dept., Univ. of Adelaide, Adelaide, Australia, 1995.
[4]Tuck, E. O., "Some Accurate Solutions of the Lifting Surface Equation," *Journal of the Australian Mathematical Society (Series B)*, Vol. 35(2), Oct. 1993, pp. 127–144.
[5]Lan, C. E., "A Quasi-Vortex-Lattice Method in Thin Wing Theory," *Journal of Aircraft*, Vol. 11, No. 9, 1974, pp. 518–527.
[6]Turrill, D., "Wings and Free Speed," *Open Wheel Magazine*, May 1992, p. 63.

Multiple Design Point Optimization of High-Speed Proprotors

Aditi Chattopadhyay,* Thomas R. McCarthy,† and Charles E. Seeley†
Arizona State University, Tempe, Arizona 85287-6106

Introduction

RECENTLY, Chattopadhyay et al.[1] developed a multilevel decomposition-based optimization procedure for improved high-speed cruise and hovering performance of tiltrotor aircraft. The goal of that study was to improve aerodynamic performance in hover and cruise in the upper level and to improve structural characteristics in these flight modes at the lower level. The aerodynamic analysis used in Ref. 1 was based on blade element approach and two-dimensional airfoil theories. These were later corroborated by Dadone et al.[2] in a parametric study conducted to investigate the important design issues associated with the development of high-speed proprotors using a comprehensive Euler analysis.

This study extends the work of Ref. 1 by including takeoff performance in the optimization formulation. The aerodynamic and structural design criteria in high-speed cruise, hover, and takeoff are addressed using a multilevel decomposition-based optimization procedure. At the upper level, the aerodynamic performance of proprotors is optimized for each flight condition using planform variables. Constraints are imposed on the rotor thrust in all three flight conditions. A nonlinear programming technique based on the Broyden–Fletcher–Goldfarb–Shanno (BFGS) algorithm is used for the optimization. At the lower level, the rotor is optimized for improved structural performance using composite ply-stacking sequence as a design variable. Since only discrete design variables are used at the lower level, an optimization procedure based on simulated annealing algorithm[3] is developed to address this complex problem. Only the major findings of this study are presented in this note and the interested reader should consult Refs. 1 and 4 for complete details of the problem formulation.

Optimization Problem

The following is a brief description of the two-level optimization problem. Detailed explanations are found in Refs. 1 and 4.

Received Dec. 29, 1995; revision received Jan. 24, 1996; accepted for publication Feb. 12, 1996.

*Associate Professor, Department of Mechanical and Aerospace Engineering, Associate Fellow AIAA.
†Graduate Research Associate, Department of Mechanical and Aerospace Engineering. Student Member AIAA.

Upper Level

The axial efficiency in high-speed cruise η_c and the figure of merit in both hover and in takeoff (FM_h and FM_t, respectively) are maximized simultaneously in this level using aerodynamic design variables. Constraints are imposed on the rotor thrust at each of these flight conditions. Geometric constraints are also imposed on the physical dimensions of the blade to ensure that the load-carrying member of the rotor is maintained within the dimensions of the airfoil. The blade is discretized and design variables include the values of chord c, twist θ, thickness-to-chord ratio t/c, and zero-lift angle of attack α_{zl} at each node. A quadratic variation with no initial offset is used to represent the lifting line to ensure continuity of the elastic axis. The parameter that determines the quadratic variation is also used as a design variable.

Lower Level

The structural characteristics of the rotor are investigated at this level. The objectives are to minimize the tip displacements in cruise, hover, and takeoff. The most critical of these displacements are included in the formulation. In cruise, the elastic twist ϕ_c and the in-plane displacement v_c are critical. In hover and in takeoff conditions, the vertical displacement (w_h and w_t, respectively), and the elastic twist (ϕ_h and ϕ_t, respectively), are significant. Therefore, these six displacements are selected as the individual objective functions to be minimized. Ply orientations are used as design variables. However, to avoid impractical values the ply angles are chosen from a set of preselected values (0, ±15, ±30, . . . , 90 deg). Stress constraints are imposed based on the Tsai-Wu failure criterion[5] on each lamina at each of the four corners of the box beam to prevent failure because of stresses.

Results

The reference rotor used is an existing advanced three-bladed gimballed rotor.[6] The aerodynamic optimization in high-speed cruise is performed at a cruise altitude of 25,000 ft and a forward velocity of 300 kn with a rotational speed of 421 rpm. A vehicle weight of 13,000 lb and aircraft lift-to-drag ratio L/D of 8.4 is assumed. Therefore, the thrust in cruise is constrained to be 774 lb for the two-engine aircraft. In hover, the aircraft is assumed to be operating at sea level conditions with a rotational speed of 570 rpm and a 12% download effect from the rotor/wing interaction. The thrust in hover is therefore constrained to be at 7280 lb. To simulate the takeoff condition a load factor of 1.25 is used. Inclusion of the 12% download effect results in a takeoff thrust of 9100 lb. A rotational speed of 570 rpm is used and an altitude of 6695 ft is assumed to simulate a high-altitude takeoff. A composite rotor blade made of Carbon-PEEK AS4/APC2 (Ref. 7) is used. The blade is discretized into 10 segments.

The nodal values of c, θ, α_{zl}, and t/c are used as design variables at the upper level. The sweep distribution Λ is based on a quadratic lifting line. This yields a total of 45 design variables. An in-house code based on the Kreisselmeier–Steinhauser (K–S) function, developed at Arizona State University,[4] is used as the optimization algorithm at this level. The search direction used during optimization is based on the BFGS algorithm[8] and the two-point exponential expansion is used to approximate the objective functions and constraints.

At the lower level, the design variables used represent discrete values of the composite ply orientations. A symmetric and balanced lay-up is assumed in both the vertical and the horizontal walls. This leads to 12 independent design variables that can assume any one of the seven preselected values of ply-angle orientations. The results from this multiple design point optimization are presented in Table 1 and Figs. 1a–1d.

The upper level objective functions are presented in Table 1. The figures of merit in hover FM_h and in takeoff FM_t are increased by 6.9 and 31%, respectively, from the reference values. A small increase (0.52%) is obtained in the cruise pro-